10th International Conference on Composite Science and Technology
ICCST/10
A.L. Araúo, J.R. Correia, C.M. Mota Soares, et al. (Editors)


# Passive Control of Aerodynamic Load in Wind Turbine Blades

**E. S. Carrolo*, A. C. Marta***

* CCTAE, IDMEC, Instituto Superior Técnico, Universidade de Lisboa
Av. Rovisco Pais 1, 1049-001 Lisboa, Portugal

edgar.carrolo@outlook.com
andre.marta@tecnico.ulisboa.pt

**Keywords:** Aeroelastic tailoring, Bend-twist coupling, Passive control, Fluid-structure interaction.

**Summary:** *Large wind turbine blades have many advantages in terms of power efficiency, despite representing an hazard concerning the high loads applied on the structure. Since the end of the last century, some researchers have been discussing about passive control techniques. The implementation of this kind of aeroelastic response does not bring additional maintenance or weight, unlike active control, because there are no additional devices or complementary structures, and is very useful either to reduce fatigue loads or optimize energy output. The main purpose was to achieve an effective reduction in aerodynamic loading in a wind turbine blade applying the concept of bend-twist coupling. In the scope of this work, computational models were developed that simulated the fluid-structure interaction on a enhanced blade model. Coupled analysis demonstrated that this design can reduce aerodynamic load and maximum tip deflection in high wind speeds, thus proving to be a realistic passive control technique.*

## 1. INTRODUCTION

Until the last quarter of twentieth century, there was in general, little interest to yield electrical energy from wind. Since then, several factors contributed to a different view about the use of wind energy. The dramatic rise of oil price forced all entities to seek for alternatives. The wind energy seemed to be a logical investment, and associated with adequate government policies made these devices proliferate in Europe and North America.

With design focused on turbine mass and cost, it is important to include control techniques to improve the turbine performance and mitigate both stress and load on the structure since, whenever a turbine blade is subjected to adverse atmospheric conditions. In this context, through aerodynamic load control is possible to manage the amount of load carried by the structure, reduce the fatigue damage and thereby enhance the overall efficiency [1]. Passive approach is privileged in sacrifice of active control, since it provides an effective blade unloading without any additional moving parts, in contrast with what happens in active control. The obvious conclusion is that is possible to achieve significant savings in weight and maintenance cost [2, 3].

For a long time, wind turbine blades have been built with composite materials, which brings a new set of opportunities regarding the anisotropic properties of those materials, in the form of aeroelastic tailoring [4], where directional stiffness is designed into the structural to control the aeroelastic deformation in a beneficial way.

Goeij et al.[3] studied two different blade configurations. The initial assumptions behind their work is that the blade deforms as reaction to the wind incidence, so it both bends (pure bending) and twist around the rotor axis. It can twist either in direction to stall, which means that exists an increase in the angle of attack or in direction to feather, that represents a decrease in the angle of attack. Bend-twist coupling (BTC) can be obtained with a base design that

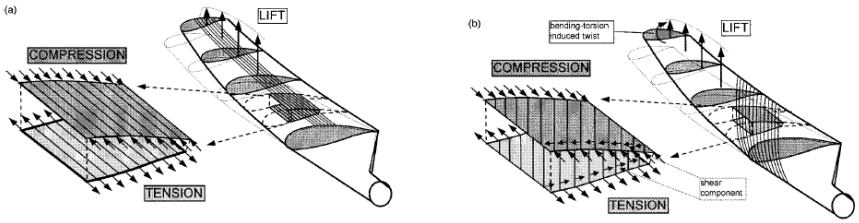


Figure 1. Comparison of a) conventional blade; b) bending-twist coupled blade [3].

includes sweep along the blade. This design creates a moment that induces twist on the blade. Another possible solution is to deviate the composite fibers out of principal axis, sufficiently to generate twist motion and decrease the load applied, as shown in Fig. 1.

A very recent study [5], working under the latter assumption, investigated the implementation of unbalanced symmetrical stacks of composite layers. The results obtained showed that unbalanced stacks cause higher levels of BTC. The BTC can be quantified from the simplified reduced cross section stiffness matrix,

$$\begin{bmatrix} EI & -S \\ -S & GJ \end{bmatrix} \begin{bmatrix} k_b \\ k_t \end{bmatrix} = \begin{bmatrix} M_b \\ M_t \end{bmatrix}, \qquad \beta = \frac{-S}{\sqrt{EI \cdot GJ}} \quad 0 < \beta < 1. \tag{1}$$

where $EI$ and $GJ$ are bending and torsional stiffness, respectively, $k_b$ is the bending curvature, $k_t$ is the rate of twist, $M_b$ and $M_t$ are bending and torsional moments, respectively, $S$ is the coupling stiffness, and $\beta$ is the normalized BTC coefficient.

## 2. AERODYNAMIC MODEL

In this work, the aerodynamic force computation is automated for a given wind speed using a custom developed numerical tool coded in $MATLAB^{®}$, following the Blade Element Method (BEM) [6, 7], that predicts the pressure distribution on the blade surface. The BEM model estimates the airfoil section 2-D aerodynamic data using a panel method, for potential flow conditions. The airfoil analysis at a blade position $r$ in BEM is done at the effective angle-of-attack given by

$$\theta_r = \theta_{0_r} + \theta_{a.c.r} + \beta_r, \tag{2}$$

where $\theta_{0_r}$ is the designed twist angle and it is a section property (so its value remains constant), $\theta_{a.c._r}$ is the active control pitch angle (it also remains constant during all iterations but should be set in the beginning of the simulation), and $\beta_r$ is the twist of structural reaction. In each solution of BEM, $\theta_r$ remains constant, but will vary due to surface deformation, whenever both aerodynamic and structural models are coupled.

The aerodynamic load on a given panel element $j$ in a blade position $r$ is directly obtained from the pressure distribution evaluated in BEM,

$$p_{r,j} = C_{p_{r,j}} \frac{1}{2} \rho U^2 + p_0, \tag{3}$$

where $p_{r,j}$ is the pressure, $C_{p_{r,j}}$ is the pressure coefficient, $U$ the wind velocity and $p_0$ is the atmospheric pressure. The pressure due to the fluid-interaction is given by dropping $p_0$.

## 3. STRUCTURAL MODEL

The numerical tool used for the structural analysis uses the Finite Element Model (FEM). The FEM solution seeks to find the minimum total potential energy $\Pi$:

$$\Pi = \frac{\partial}{\partial q} \left( \int_V \frac{1}{2} \{\varepsilon\}^T \{\sigma\} dv \right) - \frac{\partial}{\partial q} \left( \int_V \{u\}^T p^V dV \right) - \frac{\partial}{\partial q} \left( \int_S \{u\}^T \{p^S\} dS \right). \tag{4}$$

Computing the strains and stress relations, differentiating relative to the nodal displacement $q$, and integrating over an element yields [8]

$$[K]\{q\} = \{f\}, \qquad \{f\} = \{p\} + \{h\}. \tag{5}$$

where the matrix $[K]$ is called element stiffness matrix, $\{f\}$ and is the load vector. Once obtained all element equations, they are assemble to form the global system of equations,

$$[K^G]\{Q^G\} = \{F^G\}., \tag{6}$$

The numerical code developed in $MATLAB^{®}$ builds, from a set of inputs defined by the user and airfoil section coordinates, a structured mesh of a wind turbine blade.

The amount of data collected to build the blade geometry assumes a special relevance, namely the number of airfoil sections collected to build it. The accuracy in the interpolation is improved if more sections are loaded. Similarly, it is also important to have a sufficiently large number of points per airfoil file, as it may affect negatively the interpolation of intermediate chord coordinates. Nevertheless, the user has freedom to choose the number of divisions in chord, span and webs, then from the set of computed airfoil sections, all nodes are generated by linear interpolations of two neighbor sections.

The nodes are then connected to form the finite element. The element chosen was *SHELL181*, that is the one most suitable to model shell structures, a bi-linear element constituted by four nodes. Special attention was given to the order of the nodes in each element to properly define the outer unitary normal vector in $ANSYS^{®}$. That fact is determinant to compute surface

loads, since a positive pressure load is applied in the opposite direction of the element unitary normal vector. Furthermore, in case of using composite materials, the stack sequence is oriented according the orientation of this vector.

The $MATLAB^{®}$ code then outputs a file with *APDL* code to be processed by the FEM tool $ANSYS^{®}$, to perform the static analysis to simulate the blade structural response.

## 4. FLUID-STRUCTURE INTERACTION MODEL

The critical point of fluid structure interaction is the transfer of information between aerodynamic and structural grids, in particular, transfer the aerodynamic load to the structural grid and the displacement field to the aerodynamic grid. The main criterion that should be guaranteed is that both aerodynamic and structural meshes are flawlessly connected, thus

$$u_{s_k} = u_{a_k}, \tag{7}$$

where $u_{s_k}$ is the position vector of an arbitrary node of the structural grid and $u_{s_k}$ is the similar accounting the aerodynamic grid.

The structural solver should be able to solve the equation of motion,

$$[M]\{\ddot{q}\} + [G]\{\dot{q}\} + [K]\{q\} = \{F\}, \tag{8}$$

where $[M]$, $[G]$ and $[K]$ are the mass, gyroscopic and stiffness matrices, and $\{F\}$ is the force vector. Under steady wind conditions, the blade is subjected to a constant aerodynamic load and the motion equation resumes to Eq.(6). The force vector $\{F\}$ contains different contributions:

$$\{F\} = \{F_0\} + \{F_g\} + \{F_{aero}\} + \{F_{n.l.}\} \tag{9}$$

where $\{F_0\}$ is the constant force, $\{F_g\}$ is the gravitational load, $\{F_{aero}\}$ is the aerodynamic load and $\{F_{n.l.}\}$ is the non-linear component. Assuming that the only constant force is $\{F_{aero}\}$, and neglecting $\{F_{n.l.}\}$ and $\{F_g\}$, the static equilibrium is given by

$$[K]\{q\} = \{F_{aero}\}, \tag{10}$$

which has the same meaning of Eq.(5). The aerodynamic vector $\{F_{aero}\}$ is obtained from the aerodynamic module.

Yu and Kwon [9] presented one simple loose coupling FSI (fluid-structure interaction) method of simple implementation. It consists on a static FSI model running in sequence both structural and aerodynamic models, the former assisted by a computational fluid dynamics (CFD) tool. The structural mesh is initially undeformed and the CFD tool calculates the aerodynamic load for the undeformed structure. Then, the output of the CFD solver is coupled to the FEM tool that will apply the aerodynamic load on the deformed mesh and provide a new output relatively to an updated deformed mesh, which will be returned in CFD solver. The iterative process is repeated until the convergence of $\{F_{aero}\}$ and displacement vector $\{q\}$ have been verified.

Since the objective of this work is to observe load mitigation due to the BTC, in this model only twist is coupled, whereas in a conventional FSI coupling model, both displacements and rotations are coupled. Thus, the load mitigation will be achieved exclusively by the variation in twist.

The coupling is initiated by the FEM tool. The aerodynamic load is treated in $ANSYS^{®}$ as a pressure load on the elements and both aerodynamic and structural meshes are coincident, as stated by Eq.(7). $ANSYS^{®}$ simulation consists in a steady static analysis of the structure and the the nodal displacement field is returned to the $MATLAB^{®}$.

From the nodal displacements, it is possible to infer about the amount of twist that the blade is subjected. A correct twist computation would be calculating it in relation to the elastic axis, however it is not possible to determine precisely where it is located. Therefore this angle was calculated taking into account the displacement of leading and trailing edges in each span coordinate,

$$\beta_i = arctan\left[\frac{(y_{i_{l.e.}} - y_{0_{l.e.}}) - (y_{i_{t.e.}} - y_{0_{t.e.}})}{(x_{i_{l.e.}} - x_{0_{l.e.}}) - (x_{i_{t.e.}} - x_{0_{t.e.}})}\right], \tag{11}$$

where $y_{i_{l.e.}}$ is the $y$ position of the leading edge in the deformed mesh, $y_{0_{l.e.}}$ is the $y$ position of the leading edge in the undeformed mesh, $y_{i_{t.e.}}$ is the $y$ position of the trailing edge in the deformed mesh and $y_{0_{t.e.}}$ is the $y$ position of the trailing edge in the undeformed mesh. The same notation is applied to $x_{i_{l.e.}}$, $x_{0_{l.e.}}$, $x_{i_{t.e.}}$ and $x_{0_{t.e.}}$ The variation of local twist is simply given by

$$\Delta\beta_i = \beta_i - \beta_{0_i}. \tag{12}$$

$\Delta\beta_i$ is updated in the BEM solver, which initially is set to zero and will make the aerodynamic load change in each iteration. The updated $\{F_{aero}\}$ is then introduced in $MATLAB^{®}$ and the iterative process is consecutively executed until $\{F_{aero}\}$ converges.

## 5. BASELINE DESIGN

### 5.1 Wind Turbine NREL 5 MW Data

The blade is constituted by a mixture of TU Delft and NACA airfoil shapes, while the root region contains circular sections. The transition region is not clearly documented. In table 1 it is possible to consult the different airfoils used in the NREL 5MW blade.

The mixture of materials commonly known as E-glass/epoxy is quite frequent in wind turbines applications, whose mechanical properties are available in table 2. This material was applied in the FEM tool, considering laminates with constant thickness, 8 layers oriented in the blade plane, +45 degrees in relation to the edgewise axis.

The free-stream wind velocity was set to 25 m/s, equal to cataloged rotor cut-out speed, and crosses the blades from the leading to the trailing edge, as usual.

| Airfoil | $[\%t/c]$ | z $[m]$) | Airfoil ID |
|---|---|---|---|
| Cylinder 1 | 100 | 1.8 | 1 |
| Cylinder 2 | 100 | 5.98 | 2 |
| DU W-405 | 40.5 | 10.15 | 3 |
| DU 97 W-300 | 35.09 | 15.00 | 4 |
| DU 91 W2-250 | 30 | 20.49 | 5 |
| DU 91-W2-250 | 25 | 26.79 | 6 |
| DU 91 W-210 | 21 | 34.22 | 7 |
| NACA 64-618 | 18 | 42.47 | 8 |

Table 1. NREL 5MW wind turbine blade airfoils [10].

| | |
|---|---|
| Density $\rho$ [kg/m$^3$] | 1920 |
| Longitudinal Modulus $E_{11}$ $[GPa]$ | 43.2 |
| Transversal Modulus $E_{22}$ $[GPa]$ | 12.6 |
| Poisson Coefficient $\nu$ | 0.38 |
| Distorsion Modulus $G$ $[GPa]$ | 4.2 |
| Yield strength $\sigma_y$ $[GPa]$ | 176.6 [1] |

Table 2. E-glass/Epoxy composite elastic properties [5].

### 5.2 Parametric Study Summary

A parametric study was done, following the implementation presentation previously. The main goal was to build an enhanced blade design that can provide the highest twist, and still maintain an acceptable global structural response. The adopted criteria to compute the enhanced design was whether it was possible exclusively from the results demonstrated from the parametric study.

The parameters under study were:

- **Fibers layers orientation**; varying initially, all fiber layers resulting in an unidirectional laminate. Then it were developed three multi-directional stacks: one balanced and two unbalanced;
- **Thickness distribution**; it was essentially compared the response between a constant distribution and two variable distributions;
- **Number of shear webs and location**; it were distinguished four different cases, where it was varied the number of webs from zero to two, and in the latter two different position were investigated, maintaining the relative distance between them constant;
- **Material reinforcement**; it was implemented besides the e-glass/epoxy composite, a

carbon fiber composite, with distinguished elastic properties in two of the most interior layers of the laminate.

All the evaluated parameters proved to be quite relevant to blade structural behavior. The fibers orientation is one parameter that might be adjusted as function of the stiffness required locally, and can provide significant improvements in the overall performance.

The thickness is probably the most sensitive and unpredictable parameter of all studied, as a refinement in specific zone must be evaluated regarding the all blade performance, avoiding the possibility of comparison of independent regions.

The influence of the number of webs was not completely clarified, but it was made clear the importance of having them in hollows structures. The structural response by single and double web configurations were very similar, so no obvious can be extracted about which one can provide the best solution according the desired proposal.

The reinforcement done with carbon fibers demonstrated in significant improvements, namely in the induced twist, whereby it is definitely a solution to consider in an enhanced design.

## 6. ENHANCED DESIGN

Following the findings in section 5, the fibers orientation should be in a such way, that can provide both flapwise stiffness and induced twist on the blade. Therefore, assuming that the blade root is subjected to high flapwise moments, it was introduced all layers with 90° fibers, (longitudinal direction), so a high longitudinal stiffness can be achieves with this layup. The root laminate stack is presented in figure 2(a).

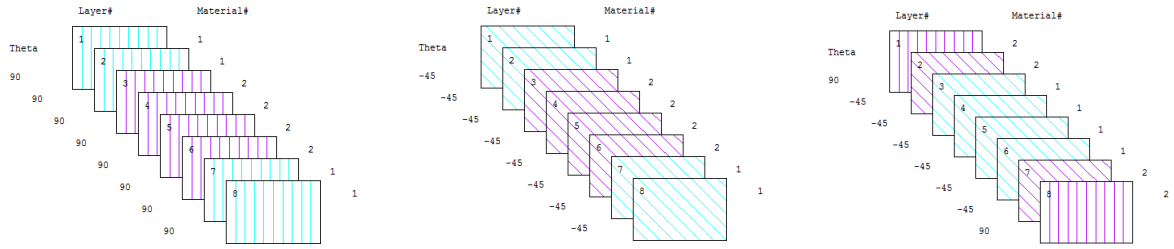


(a) Root. (b) Tip. (c) Mid-span.

Figure 2. Different laminate stacks.

Ideally, the remain blade surface should be covered by layers with -45° fibers, but buckling issues might occur and for that reason, usually real blades have layers with longitudinal fibers [11]. Hence, it was applied a stack to the blade surface as in figure 2(b). The region right next to the root, between 10 and 20m, has shown to be region of structural demand, thus two additional longitudinal fibers were replaced from -45°, creating an intermediate solution between root and tip stacks, as illustrated in figure 2(c).

The thickness distributions of figure 3 was previously tested during the parametric study. It caused a great loss of stiffness, but the author believes that the positives effects of the new laminate stack, will mitigate adverse effects of having this thickness distribution.

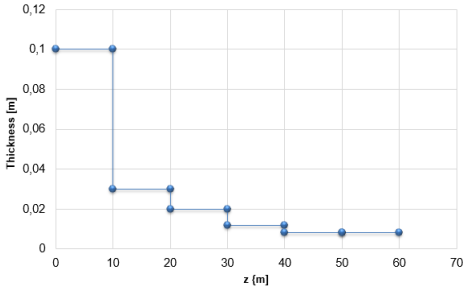


Figure 3. Enhanced blade thickness distribution.

The shear webs position was changed in relation to the baseline design, although the double web configuration has been maintained. The argument of this modification has to do with the lack of effectiveness demonstrated by the shear web located closer to the trailing edge. Despite, the good performance evidenced by the single shear web configuration, it is not clear that this performance could be consistent when a variable thickness distribution is introduced. Furthermore, in the research that supported this work, the double web configuration is rather used than single one. Further studies would be necessary to abandon this conservative solution.

Finally, regarding the reinforcement done with the composite of table 3, it revealed to be successful, and it was integrated in the laminates stack, as shown in figures 2(a) to 2(c) labeled by material 2. At the root, the interior layers were changed to carbon composite, and the remaining blade span included carbon fibers not only in the longitudinal layers but also in the interior layers containing oblique fibers.

| | |
|---|---|
| Density $\rho$ $[kg/m^3]$ | 1590 |
| Longitudinal modulus $E_{11}$ $[GPa]$ | 155 |
| Transversal modulus $E_{22}$ $[GPa]$ | 9 |
| Poisson coefficient $\nu$ | 0.3 |
| Distorsion modulus $G$ | 3.5 |
| Yield strength $\sigma_y$ $[MPa]$ | 633.4 |

Table 3. Carbon(T300)/epoxy composite mechanical properties [5].

## 7. COUPLED ANALYSIS

This analysis consisted on an iterative solution, coupling the $\Delta\beta$ into the aerodynamic model to obtain an updated surface load. The simulation has been ran until converged results have been verified. It was considered either only the aerodynamic load or the latter including the presence of inertial loads, considering in this case that the reference angular velocity is the rated rotor speed, 12 rpm.

### 7.1 Structural Performance

With five iterations it was possible to get a converged solution, regarding nodal displacements and twist distribution.

The maximum tip deflection in [11] was 8.46 m, for a rotating situation. In that work, it was being analyzed a 70 m blade, also developed by NREL, with identical geometrical features. Thus, it is acceptable to make a linear re-scaling to have a reference value about the maximum tip deflection of the blade one is working. The estimated value was 7.25 m. In [11], it was also applied a safety factor of 1.35 in all forces, but for convenience, in this analysis it was applied the same safety factor to the maximum tip deflection, yielding 5.37 m.

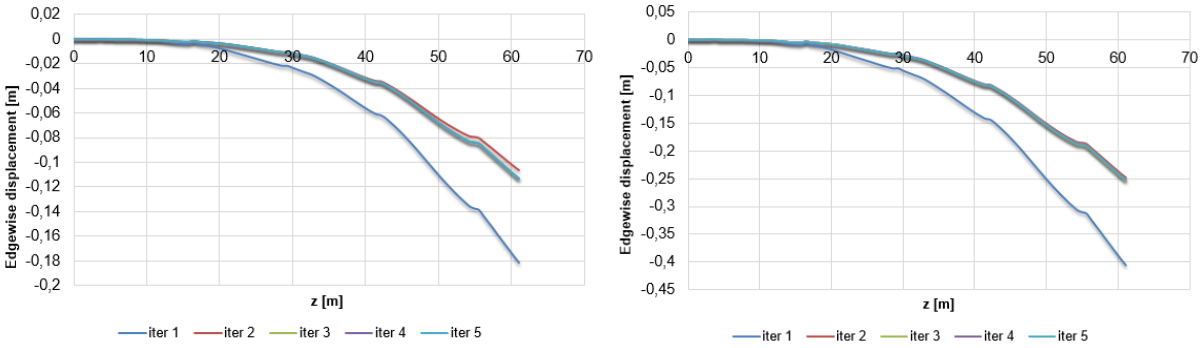


(a) Enhanced blade.

(b) Enhanced blade including inertial loads.

Figure 4. Edgewise displacement at $(^{x}/_{c}) = 25\%$.

The results show that the aerodynamic load can effectively be mitigated with this design, and produce significant reductions in both flapwise and edgwise displacement, which is visible in figures 4(a) and 5(a). The twist distribution in figure 6(a) is also lower when the solution is converged, but that difference is not so noticeable. In figures 5(b) and 4(b) is clearly visible that considering inertial loads, the total load is significantly higher, imposing much more structural demand to the blade than the former case.

The stress distribution, in figure 7(a) shows that the reinforcement applied after the root region was not sufficient to mitigate the high stresses in that region, although the maximum value is clear lower than the estimated yield strength of the composite.

The increase in total load when inertial loads were added it was reflected on the increase in the stress exerted on the blade, as shown in figure 7(b). Unlike the former analysis, the total load yields a maximum stress very close to yield strength. If the previous safety factor is applied, in fact this threshold is slightly exceeded. Similarly as what happens in figure 7(a), from the stress plot of figure 7(b) is evident an overstressed region next to the root, due not only to the insertion zone of webs, but also where high suction zones are found. Therefore, for a more conservative approach is prudent, to reinforce this zone either by changing some of the oblique layers by longitudinal layers, or alternatively make a slight adjustment in laminate thickness.

Anyway, further investigations should be done about the stress distribution concerning the

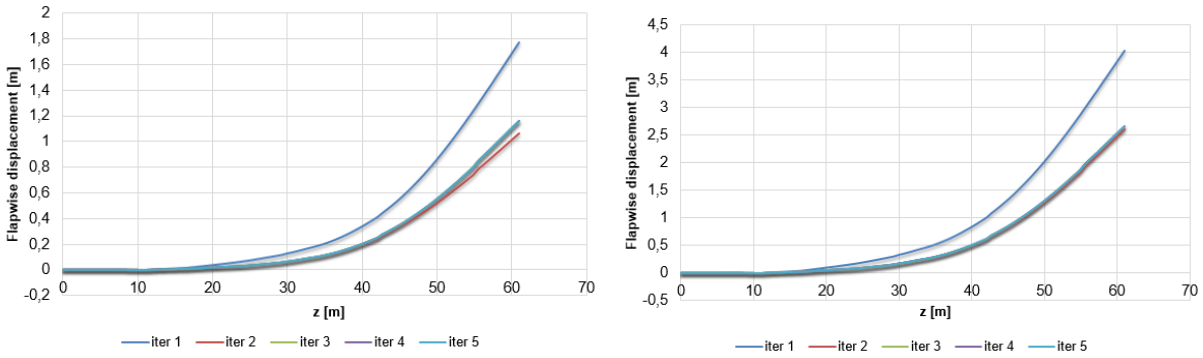


(a) Enhanced blade. (b) Enhanced blade including inertial loads.

Figure 5. Flapwise displacement at $(^{x}/_{c}) = 25\%$.

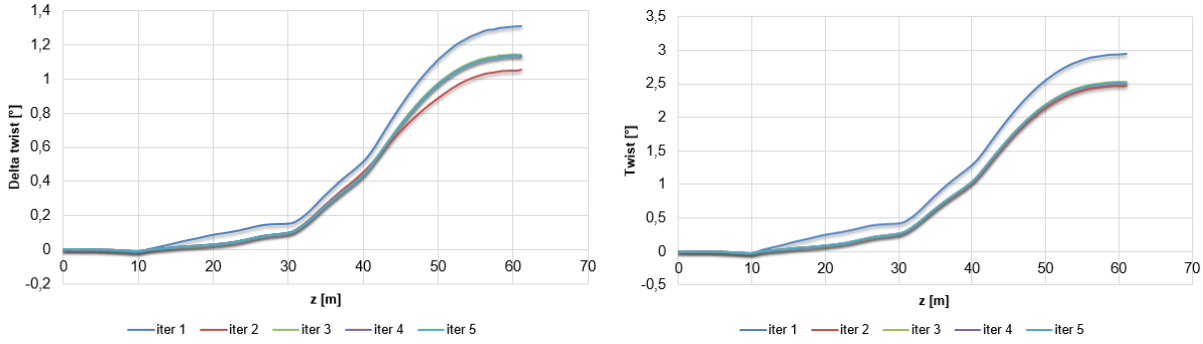


(a) Enhanced blade. (b) Enhanced blade including inertial loads.

Figure 6. Twist distribution.

implementation of BTC in WTB, as some researchers ([3], [1]) affirm that designs implemented high levels of BTC can increase fatigue loads. Therefore, the impact of this stress in fatigue lifetime should be evaluated.

The estimated initial total load in upper and lower blade surfaces, considering just the influence of aerodynamic load were

$$|F_{upper}| = 87.3\ kN \ \ and \ \ |F_{lower}| = 33.5\ kN.$$

In the end of coupled analysis, these values were

$$|F_{upper}| = 85.0\ kN \ \ and \ \ |F_{lower}| = 33.4\ kN,$$

resulting in total aerodynamic load reduction of 2.1%. This result is explicit about the interest about the mitigation of aerodynamic load since, with small savings, it is possible to achieve less demanding structural requirements.

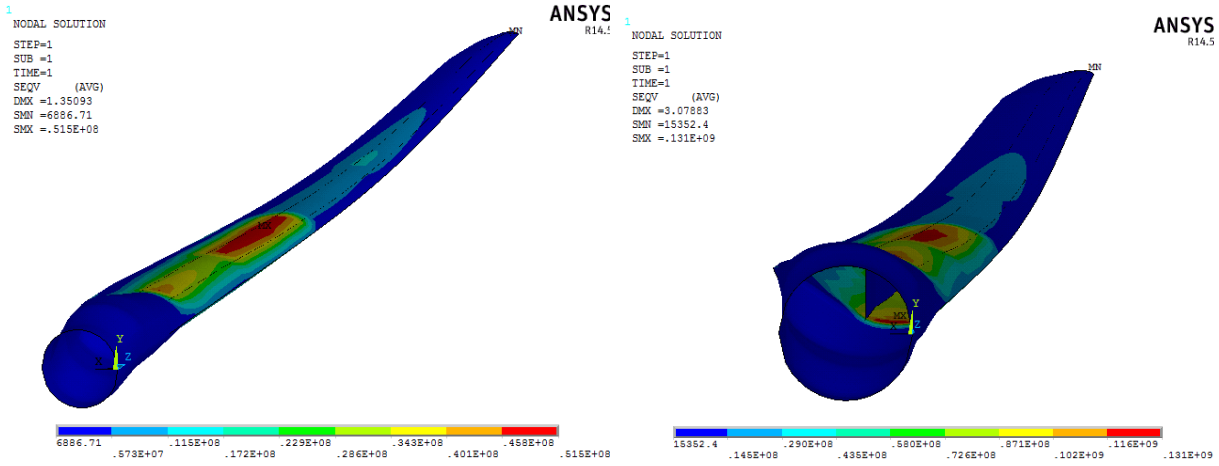


(a) Enhanced blade. (b) Enhanced blade including inertial loads.

Figure 7. von Mises stress.

## 8. CONCLUSIONS

The design presented in this work focused on a blade configuration that could provide the maximum twist possible, in a such way that applying the BTC concept could achieve an effective aerodynamic load reduction. This reduction is particularly visible in lower maximum displacements and stresses in the structure.

The developed enhanced design was justified from the conclusions of the parametric study and confirmed its proposals. Besides the reduction of total aerodynamic load through the coupling of induced self twist, both blade flapwise and edgewise maximum deflections were reduced with this design. Taking into account the reference values, and all the developed reasoning, it has been shown that the blade stiffness was correctly dimensioned, as the maximum stress ranged below the material yield strength.

The integration of inertial loads in the analysis has confirmed that these source of loads are quite relevant in design stage, as represent a significant part of total load exerted upon the blade. This design maintained enough sturdiness to keep maximum displacements below reference values, so a sort of static validation of this model was performed successfully.

## References

[1] Don W. Lobitz and Paul S. Veers. Load Mitigation with Bending/Twist-coupled Blades on Rotors using Modern Control Strategies. *Wind Energy*, 6(2):105–117, 2003. doi: 10.1002/we.74.

[2] E Muljadi, K Pierce, P Migliore, National Wind, and National Renewable. Control strategy for variable-speed Stall-Regulated Wind Turbines. *NREL Laboratories*, 1998.

[3] W.C. de Goeij, M.J.L. van Tooren, and A. Beukers. Implementation of bending-torsion

coupling in the design of a wind turbine rotor blade. *Journal of Applied Energy*, 2:191–207, 1999.

[4] Christian Deilmann. Passive aeroelastic tailoring of wind turbine blades - A numerical analysis -. Master's thesis, Massachussets Institute of Technology, 2009.

[5] Manudha T. Herath, Aaron K.L. Lee, and B. Gangadhara Prusty. Design of shape-adaptive wind turbine blades using differential stiffness bend-twist coupling. *Ocean Engineering*, 95:157–165, February 2015. doi: 10.1016/j.oceaneng.2014.12.010.

[6] Martin O. L. Hansen. *Aerodynamics of Wind Turbines*. EARTHSCAN, 2 edition, 2008. 978-1-84407-438-9.

[7] John D. Anderson. *Fundamentals of Aerodynamics*. Mc Graw Hill, 3rd edition, 2001. ISBN 0-07-237335-0.

[8] G. P. Nikishkov. *Introduction To The Finite Element Method*. Lecture Notes UCLA, 12 edition, 2004.

[9] Dong Ok Yu and Oh Joon Kwon. Predicting wind turbine blade loads and aeroelastic response using a coupled CFD-CSD method. 70:184–196, 2014. doi: 10.1016/j.renene.2014.03.033.

[10] Brian R Resor. Definition of a 5MW / 61 . 5m Wind Turbine Blade Reference Model. 2013.

[11] Kevin Cox and Andreas Echtermeyer. Structural design and analysis of a 10MW wind turbine blade. *Energy Procedia*, 24(1876):194–201, 2012. doi: 10.1016/j.egypro.2012.06.101.